Colloid Polym Sci (2007) 285:1321–1329
DOI 10.1007/s00396-007-1689-6

Non-ionic and cationic micelle nanostructures as drug solubilization vehicles: spectrofluorimetric and electrochemical studies

Elena Lorente · Alberto Rodríguez · Emilio Aicart · Elena Junquera

Received: 28 March 2007 / Accepted: 24 April 2007 / Published online: 5 June 2007

Abstract The use of colloidal organized media, such as micelles, to solubilize tetracaine hydrochloride (TC.HCl), a local anaesthetic drug, in aqueous solution has been studied by means of fluorescence spectroscopy at 298.15 K. Because tetracaine molecule is a fluorescent probe, changes in the fluorescence emission spectra of the drug when it is solubilized by the micelles enable the study of the micelles–drug association process through the calculation of the association constants. Two kinds of micelles have been selected to solubilize the drug: non-ionic micelles and cationic micelles. Complementary conductometric experiments were also done to determine the critical aggregation concentration of the surfactants in the presence of the drug. The micelle–drug association process has been also analyzed by deconvoluting the fluorescent of the drug into several Gaussian components, each of which assigned to the solubilization of the drug within different microenvironment inside and outside the cationic and/or non-ionic micelles.

Keywords Fluorescence spectroscopy · Probe emission · Self-aggregated systems · Association constants · Conductivity · Micelles · Nanoaggregates · Solubilization · Tetracaine · Drug delivery systems

E. Lorente · A. Rodríguez · E. Aicart · E. Junquera (✉)
Departamento de Química Física I, Facultad de Ciencias Químicas, Universidad Complutense de Madrid, 28040 Madrid, Spain
e-mail: junquera@quim.ucm.es
URL: http://www.ucm.es/info/coloidal/index.html

Introduction

Self-assembly colloidal structures are known to play an important role in overcoming the undesirable side effects that usually accompany the function of many drug molecules in the organism, serving as suitable drug vehicles in aqueous media [1 and 2 and references therein]. The complex molecular architectures of these lipid-based drug delivery systems can be advantageously used to facilitate solubilization, stabilization, and delivery of many drug substances. Among these self-assembly colloidal carriers, the more commonly used are micelles, microemulsions, emulsions, vesicles/liposomes, and liquid crystal nanostructures [1, 2 and references therein]. In particular, micelle aggregates, considered the simplest colloidal organized media, may solubilize the hydrophobic parts of drugs both within the micelle core or in the surface, depending on the structure of the drug molecule [1, 2]. Fluorescence spectroscopic techniques make use of this fact to analyze the solubilization phenomena of drugs that has a fluorophore group in their molecules, as it well documented the intensification of luminescent processes of lumiphors partial or totally solubilized by an organized hydrophobic media, due to the better protection from quenching and other processes occurring in the bulk solvent [3–7]. In this sense, the micelle core behaves similarly to an organic solvent; it affords an apolar environment and a non-hydrated state for the solubilized probe. The maximum fluorescence intensity is obtained from a molecule that is totally solubilized inside the micelle core, and the more a molecule is subjected to a less apolar environment, the lower its fluorescence intensity. Accordingly, the observation of steady-state emission enhancement on the fluorescence spectrum of a fluorophore in an aqueous environment, upon addition of surfactant over its critical aggregation

concentration, can be used as an indication of association. A number of references in the literature [2, 3, 8–10] use this change on the spectroscopic properties of the drug, as solubilization by the micelle aggregate occurs, to study the binding process through the association constant.

Tetracaine hydrochloride (see Scheme 1) belongs to an important class of synthetic drugs of the therapeutic family of local anesthetics whose structures resemble natural compounds actively participating in nerve-impulse transmission. It is believed that the cationic form of the drug that seems to be the active principle joins the Na^+ channels on the nerve membrane, thus, blocking the initiation and transmission of nervous impulses [11, 12]. Most of the local anesthetics that have a hydrophilic region (a tertiary or secondary amine) and a hydrophobic region (an aromatic portion), separated by an alkyl chain of the ester or amide type, often show a short duration of action, and adverse side effects, such as cardiac and neurological toxicity, accompanied sometimes by allergic reactions. It is then expected that the formulation of tetracaine hydrochloride, as solubilized in surfactant nanoaggregates, may show a better bioavailability with all or some of these undesirable effects masked or abolished.

Most of the studies reported in the literature regarding the use of lipid-based drug delivery systems are focused on their pharmacological aspects, the physicochemical standpoint being less frequent [8–10, 13–18]. In this work, we present a spectroscopic study of the solubilization of tetracaine hydrochloride by micelle aggregates, aimed at determining the association constant of the micelle–drug system. Because tetracaine molecule is a fluorescent probe due to its planar aromatic ring, the analysis is based on the measurement of the fluorescence intensity of the anesthetic drug in aqueous solutions at constant concentration in the presence of increasing surfactant and/or micelle concentration. Complementary conductometric experiments are also done to determine the critical aggregation concentration of the surfactants in the presence of the drug. Two kinds of micelles have been selected to solubilize the drug: (a) non-ionic micelles formed from a glycosilated single-chain surfactant, octyl-β-D-glucopyranoside (OBG), a non-ionic alkylglycosidic surfactant widely used in biomembrane research and reconstitution processes of biological membranes or mimetic bilayers [19–24] and of great biochemical and pharmacological importance [25–27], and (b) cationic micelles formed from dodecyltrimethylammonium bromide (C_{12}TAB), a single-chain surfactant of the alkyltrimethylammonium salts family also used in pharmaceutical applications [28].

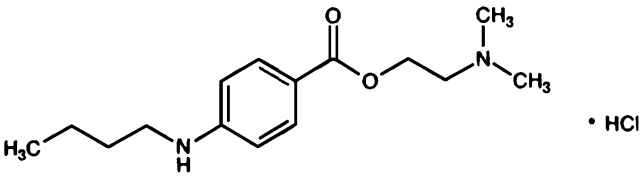

Scheme 1 Molecular structure of tetracaine hydrochloride (TC.HCl)

We believe that the results of these studies will show the convenience of characterizing this kind of associations from a physicochemical point of view to improve the understanding of the interactions in the drug–colloidal aggregates that will positively affect the design of suitable new drug delivery systems.

Experimental

Materials

The local anesthetic drug 4-(butylamino)benzoic acid 2-(dimethylamino)ethyl ester monohydrochloride, usually named tetracaine hydrochloride (TC.HCl), the non-ionic surfactant OBG, and the cationic surfactant dodecyltrimethylammonium bromide (C_{12}TAB) were from Sigma, the purities being higher than 99% for the drug and higher than 98% for the two surfactants. All were used without further purification. Distilled water was deionized using a Super Q millipore system (with a conductivity lower than 18 μS cm^{-1}) and, finally, was also degassed with a vacuum pump before the preparation of the solutions. The drug is an ester of the *p*-aminobenzoic acid that may suffer hydrolysis in aqueous media. Additionally, its cationic form (TCH^+) is in equilibrium with its non-ionized form (TC). The pH of the aqueous solutions of TC.HCl, measured as a function of drug concentration at 25 °C with a computerized procedure described previously [29], revealed (pK_a=8.4) that the ester is not hydrolyzed in aqueous solution with the concentration ranges used herein and that the above-mentioned equilibrium is almost totally shifted toward the ionized form of the drug with a negligible contribution of the non-ionized form. For that reason, unbuffered drug solutions were used in all the experiments reported herein.

Fluorescence spectroscopy

Steady-state fluorescence experiments were carried out with a Perkin–Elmer LS-50B luminescence spectrometer equipped with a xenon discharged lamp equivalent to 20 kW for 8-μs duration, with a pulse of FWHM (full width half maximum) <10 μs and a frequency of 50 Hz, and a Monk–Gillieson monochromator that may scan the excitation from $200<\lambda_{exc}<800$ nm and the emission from $200<\lambda_{em}<900$ nm, with a resolution of 0.5 nm [30, 31]. A 10-mm stoppered rectangular silica cell was placed in a stirred cuvette holder whose temperature was kept constant at 298.15±0.01 K with a recirculating water circuit. An excitation wavelength of 305 nm was chosen, and the emission wavelength was

varied from 315 to 500 nm to record the fluorescent emission of tetracaine. In all the cases, excitation and emission band slits were fixed at 2.5 nm, and the scan rate selected at 240 nm/min. Following a procedure previously detailed [32, 33], the experiments were done as a function of nanoaggregates concentration at a constant drug concentration. All the spectra used in the analysis of this work were obtained by discounting from the measured spectra (tetracaine/surfactant/water solution) the corresponding blank spectra (surfactant solution of the same concentration but in the absence of tetracaine).

Conductometry

Conductivity data were collected at 298.15 K (±1 mK) with a Hewlett–Packard 4263A LCR meter, using a Metrohm electrode whose calibration with a KCl standard solution yields a cell constant of 0.8084 cm^{-1}. Mixtures were prepared from a Metrohm digital burette, whose cylinder was kept at the same constant temperature of the measuring cell. The conductometer and the burette were controlled via IEEE-488 bus and RS-232C interfaces, respectively, with a QuickBasic software designed by us. The whole equipment, the preparation of mixtures, and the fully computerized procedure was widely described previously [34]. The accuracy on the specific conductivity, κ, obtained as an average of 2,400 measurements for each concentration, is better than 0.03%. The conductivity measurements were made as a function of surfactant concentration at constant drug concentration.

Results and discussion

When a surfactant that forms self-aggregates is added to a drug aqueous solution at concentrations over the critical aggregation concentration, the drug may be solubilized within the micelle aggregate with the establishment of an equilibrium between the free and solubilized/associated drug as follows:

$$\text{micelle} + \text{drug} \underset{}{\overset{K}{\rightleftharpoons}} \text{micelle:drug} \tag{1}$$

the association constant, K, being expressed as

$$K = \frac{[MIC:Drug]}{[MIC][Drug]_{free}} = \frac{a}{b}[MIC]^{-1}, \tag{2}$$

where MIC is the abbreviation used herein for micelles.

In Eq. 2, a and b are the molar fraction of the drug in the aggregate and in the solvent, respectively, and [MIC] the concentration of micelles defined as

$$[MIC] = \frac{[S]^{agg}}{N_{agg}} = \frac{[S]_{tot} - CMC}{N_{agg}}, \tag{3}$$

where $[S]_{tot}$ is the total concentration of the surfactant, $[S]^{agg}$ is the concentration of the aggregated surfactant, CMC is the critical aggregate concentration of the surfactant in the micelle/drug system, and N_{agg} is the aggregation number. Several physicochemical properties can be used to determine the association constant, as long as the property is sensible to the association phenomena being studied. If the property is the intensity, I, of the fluorescence emission of the drug immersed within the micelle microenvironment, a method of measuring the distribution of the drug between the water and the micelle phase (the a/b ratio in Eq. 2) is based on the fact that the lifetime of the fluorescent probe in the micelle is different than that in water. By changing the ratios of associated to free probe, the equilibrium constant can be obtained by fitting the experimental fluorescence intensity results to the well-known linearized form of the fluorescence-binding isotherm [3]:

$$\frac{1}{(I - I_0)} = \frac{1}{(I_\infty - I_0)} + \frac{1}{(I_\infty - I_0)K[MIC]} \tag{4}$$

where I_o and I_∞ are the fluorescence intensity of the drug in the absence of micelles and when all the drug is solubilized within the aggregate, respectively. If the plot of $(I-I_o)^{-1}$ vs $[MIC]^{-1}$ is linear, the slope and intercept of this plot according to Eq. 4 permit to obtain I_∞ and K as parameters of the fit. On the contrary, nonlinear regression methods are highly recommended.

To apply the above-mentioned equations, several micelle parameters should be known, such as CMC and N_{agg}. OBG and C_{12}TAB are well-known non-ionic and cationic surfactants, respectively, that forms micelles at a certain concentration. In the case of OBG, as both monomers and micelles are non-ionic, its self-aggregation can not be studied with conductometric techniques; other nonelectrochemical methods, such as surface tension or speed of sound must be used [31, 35]. However, if an ionic substrate, as is the case of tetracaine, is present, the potential association/solubilization of the drug by the OBG micelles can be analyzed by running conductometric experiments, as is also the case of cationic C_{12}TAB micelles. Figures 1 and 2 collect the conductivity values, κ, of aqueous solutions of tetracaine (at constant concentration of 1.95 and 4.87 mM, respectively) as a function of surfactant concentration. As expected, κ remains constant in Fig. 1 with [OBG] up to its micelle aggregation, but after the micelles are formed, it decreases, indicating a clear association of tetracaine to the

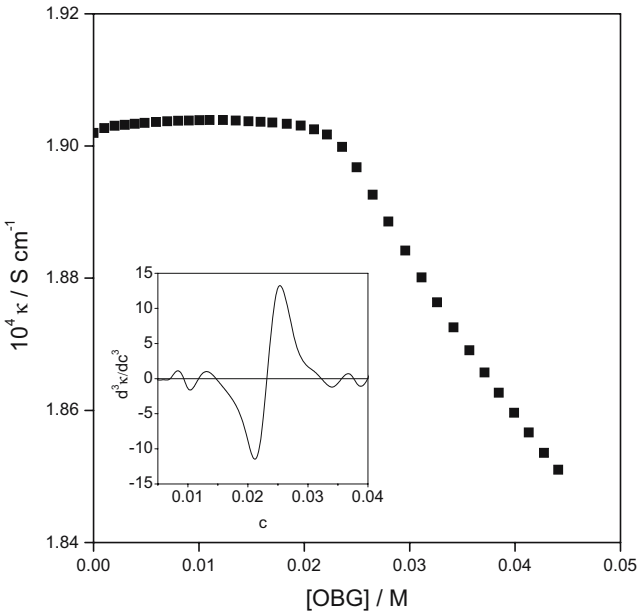

Fig. 1 Plot of conductivity, κ, as a function of octyl-β-glucopyranoside concentration, [*OBG*], at constant concentration of tetracaine hydrochloride ([TC.HCl]=1.95 mM). The *inset at the bottom* shows the third derivative of conductivity with respect to the concentration (Phillips plot)

OBG non-ionic micelles that leads to a decrease on its mobility. In the case of cationic C_{12}TAB (Fig. 2), because both drug and surfactant are ionic, the conductivity always increases with surfactant concentration but with a different slope when C_{12}TAB micelles are formed in the presence of a constant tetracaine concentration. The breaks shown by κ

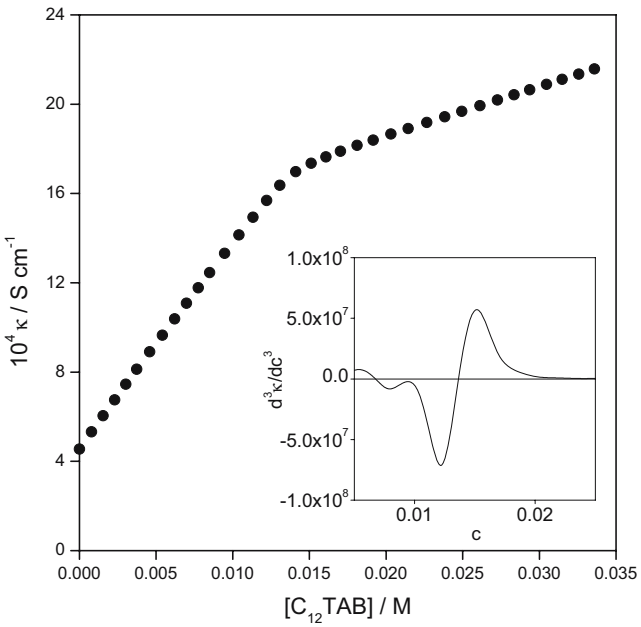

Fig. 2 Plot of conductivity, κ, as a function of dodecyltrimethylammonium bromide concentration, [C_{12}TAB], at constant concentration of tetracaine hydrochloride ([TC.HCl]=4.87 mM). The *inset at the bottom* shows the third derivative of conductivity with respect to the concentration (Phillips plot)

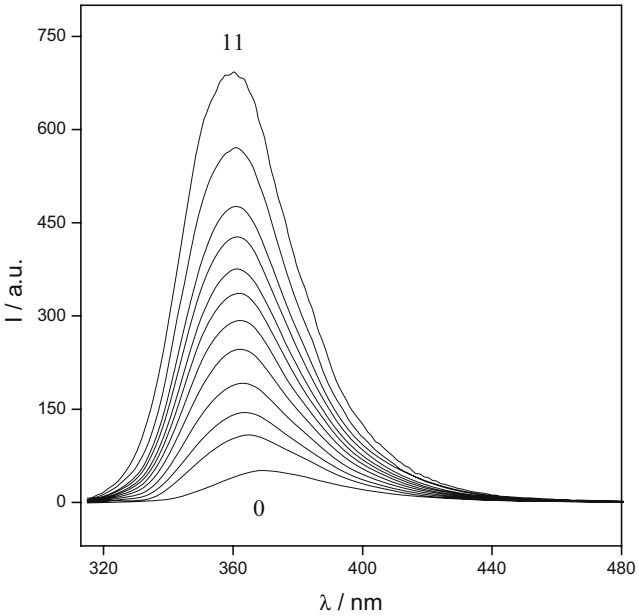

Fig. 3 Emission fluorescence spectra of tetracaine hydrochloride ([TC.HCl]=5.45 μM) immersed on aqueous solutions of OBG at increasing surfactant concentration: *curve 0* 0 mM, *curve 1* 31.50 mM, *curve 2* 34.44 mM, *curve 3* 38.39 mM, *curve 4* 42.96 mM, *curve 5* 47.44 mM, *curve 6* 51.86 mM, *curve 7* 55.58 mM, *curve 8* 60.93 mM, *curve 9* 67.41 mM, *curve 10* 72.95 mM, and *curve 11* 99.01 mM

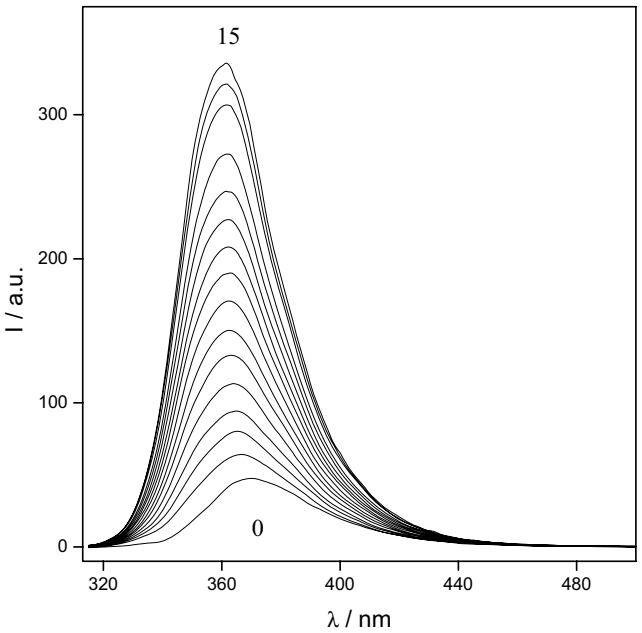

Fig. 4 Emission fluorescence spectra of tetracaine hydrochloride ([TC.HCl]=5.45 μM) immersed on aqueous solutions of C_{12}TAB at increasing surfactant concentration: *curve 0* 0 mM, *curve 1* 20.37 mM, *curve 2* 22.50 mM, *curve 3* 25.04 mM, *curve 4* 27.92 mM, *curve 5* 31.06 mM, *curve 6* 34.39 mM, *curve 7* 37.85 mM, *curve 8* 41.38 mM, *curve 9* 44.92 mM, *curve 10* 48.43 mM, *curve 11* 51.87 mM, *curve 12* 55.23 mM, *curve 13* 61.58 mM, *curve 14* 64.55 mM, and *curve 15* 67.38 mM

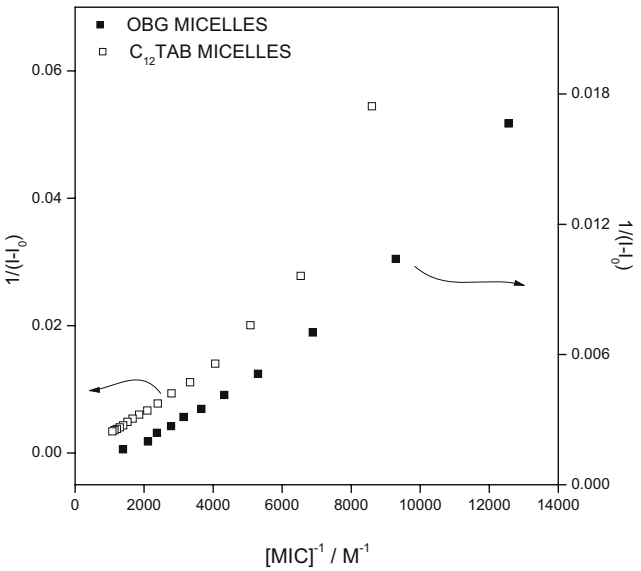

Fig. 5 Plot of $1/(I-I_0)$ vs $[MIC]^{-1}$ (where $[MIC]^{-1}$ represents the inverse micelle concentration) for OBG and/or $C_{12}TAB$ micelle solutions at constant tetracaine hydrochloride concentration, [TC.HCl]=5.45 μM

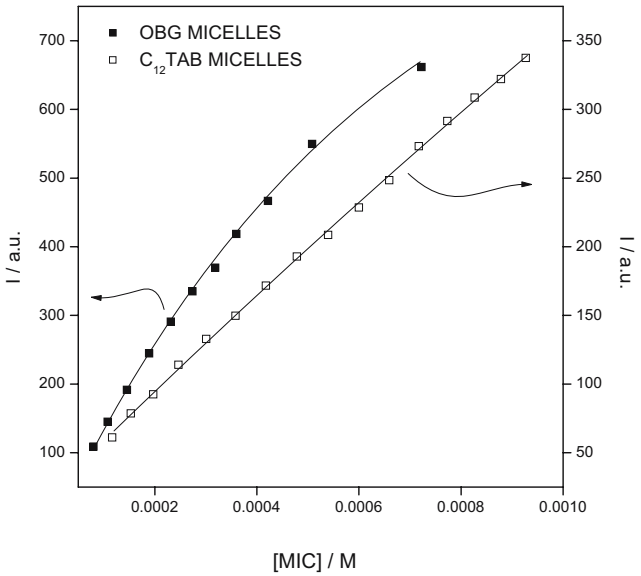

Fig. 6 Plot of the emission fluorescence intensity, *I*, of tetracaine hydrochloride ([TC.HCl]=5.45 μM) vs [MIC], (where [*MIC*] represents the micelle concentration of OBG and/or $C_{12}TAB$)

in Figs. 1 and 2 correspond to the critical aggregation concentration of OBG and $C_{12}TAB$ in the presence of tetracaine and have been determined with Phillips plots [36], i.e., as the concentrations at which the third derivative of the experimental property is equal to zero ($\frac{\partial^3 \kappa}{\partial c^3} = 0$; see the insets in the figures). Values of CMC=23.1 mM and CMC=13.64 mM has been respectively obtained for OBG and $C_{12}TAB$ in the presence of tetracaine.

Once the solubilization of tetracaine by either nonionic or cationic micelles has been confirmed, we have used the fluorescence spectroscopic technique to determine the association constants. Figures 3 and 4 show the effect of the addition of OBG and/or $C_{12}TAB$ on the fluorescence emission spectra of tetracaine in aqueous solution at a constant concentration of 5.45 μM. As can be seen in the figures, the increase on surfactant concentration (always above CMC) leads to clear emission intensity enhancements, pointing again to a solubilization/association of the drug within the micelle in a microenvironment that has to be more hydrophobic than the bulk solvent. Aiming at determining the association constant between the nonionic and/or cationic micelles and the drug, the quantities $1/(I-I_0)$, where I are the experimental fluorescence intensity values at λ=362 nm (which is the λ_{max}±3 nm for all the spectra), have been plotted in Fig. 5 as a function of the inverse micelle concentration, 1/[MIC]. The micelle aggregation numbers, N_{agg}=105 for OBG and N_{agg}=58 for $C_{12}TAB$, necessary to obtain [MIC] with Eq. 3 have been previously determined in our laboratory from static fluorescence experiments, using pyrene as fluorescent probe and hexadecylpyridinium chloride as static quencher [31]. As can be clearly seen, the plots in Fig. 5 are not linear, revealing that Eq. 4 is not valid for the analysis of the solubilization of tetracaine neither in non-ionic OBG micelles nor in cationic $C_{12}TAB$ micelles. In these cases, non-linear regression fits of I vs [MIC] data, shown in Fig. 6, are usually recommended. The equation that best fits the experimental data on this figure is

$$I = I_\infty - (I_\infty - I_0)\, e^{-K[MIC]}, \qquad (5)$$

where I_∞ and K can be obtained as nonlinear regression fit parameters. The fitted curves confirm the goodness of the

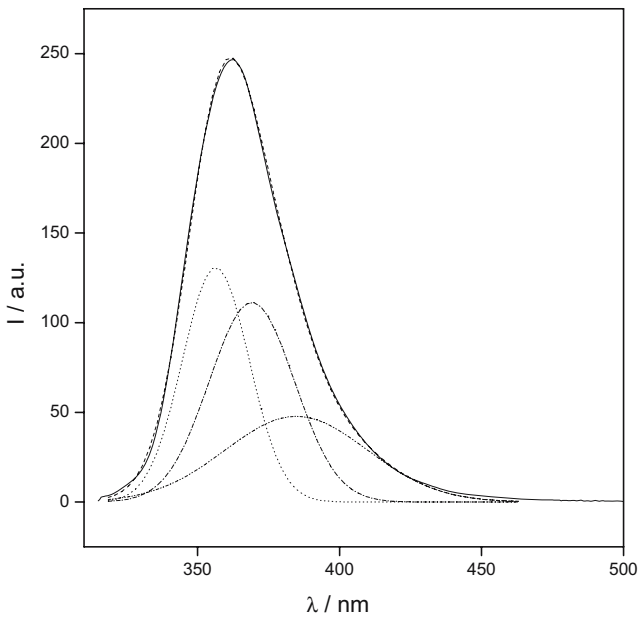

Fig. 7 Deconvolution of the emission fluorescence band of tetracaine hydrochloride immersed on a micelle solution of OBG ([OBG]=42.96 mM) on three Gaussian components

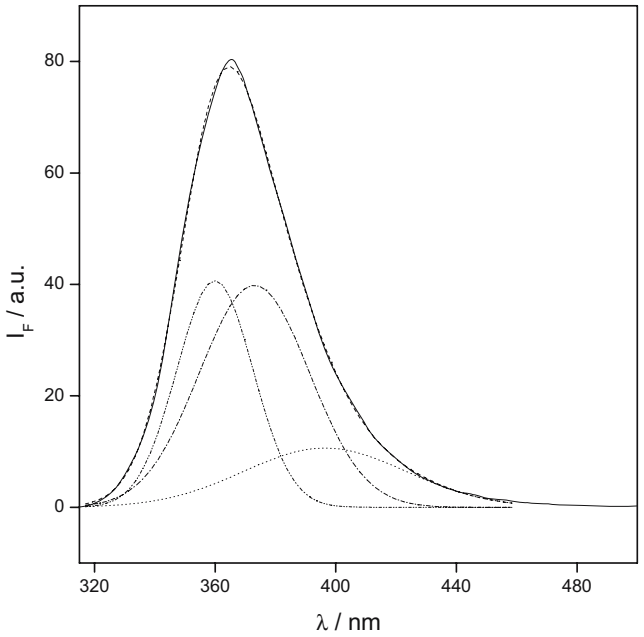

Fig. 8 Deconvolution of the emission fluorescence band of tetracaine hydrochloride immersed on a micelle solution of OBG ([C_{12}TAB]= 22.50 mM) on three Gaussian components

procedure (r^2>0.999) that gives values of $K_{TCH^{\pm}OBG} = (1,560 \pm 260)M^{-1}$ and$K_{TCH^{\pm}C12TAB} = (170 \pm 70)M^{-1}$ for the association constant of tetracaine with OBG non-ionic micelles and C_{12}TAB cationic micelles, respectively.

It is well-known [1, 4] that, as long as the organism "makes use" of a drug, the equilibrium shown by Eq. 1 is shifted by mass action toward the release of the active principle, keeping and regulating its presence in the medium. This controlled delivery has advantages that can be resumed as follows: (1) the adverse side effects can be substantially reduced because the quantity of drug that is really free and available in the medium may be much lower than the administered dose and (2) the time of action of the drug can be prolonged, which in the case of most drugs, is particularly important given its well-known fast onset of action and subsequent short elimination half-life. It is evident that the value of the association constant of the drug/micelle complex depends on the characteristics of the micelle aggregate and the drug to be solubilized, and this overall affinity involves a particular balance between the different noncovalent intermolecular forces that take place in the association process, i.e., van der Waals contacts, electrostatic and hydrophobic interactions, hydrogen bonds, solvation processes, etc. It is, then, necessary to determine these association constants and to choose the optimum vector for each specific drug. Association constant values ranging from 100 to 10,000 M^{-1} are found to be appropriate [1, 5, 37], as they enable the above described controlled release of the drug. In this sense, the association constants obtained in this work for the tetracaine/OBG micelles and for tetracaine/C_{12}TAB micelles fall within the optimum range, with moderate values, indicating that the micelles studied herein are suitable vehicles to solubilize and transport the local anesthetic drug tetracaine. In particular, OBG nonionic micelles seem to be more appropriate as tetracaine carrier than C_{12}TAB cationic micelles, mostly due to the following: (1) The corresponding binding constant is higher, and (2) the toxicity of the OBG surfactant is less, widely used in biomembrane research [19–24].

Additionally, the association process of the fluorescent tetracaine with the micelles has been also analyzed in terms of the characteristics of the different Gaussian components in which the global $\pi \rightarrow \pi^*$ emission band can be deconvoluted. Among others [7, 38], the approach used in this work interprets the mechanism by which the excited state is formed and deactivated considering that most of the $\pi \rightarrow \pi^*$ emission bands consist of several bands, attributed

Table 1 Parameters of the deconvoluted Gaussian components of the fluorescence emission of tetracaine (TC.HCl) in aqueous solutions at constant concentration ([TC.HCl]=5.45 μM) in the presence of OBG at various micelle concentrations: wavelength λ_t, width W_i, area A_i, and percent contribution to the overall fluorescence emission area (within the parenthesis)

[OBG] (mM)	[MIC] (mM)	λ_{max} (nm)	I_{362}	λ_1 (nm)	W_1	A_1 (%)	λ_2 (nm)	W_2	A_2 (%)	λ_3 (nm)	W_3	A_3 (%)
31.50	0.080	365	109	357	23	1,798 (37)	372	30	2,153 (43)	389	49	1,008 (20)
34.44	0.108	364	145	357	24	2,533 (38)	372	31	2,774 (42)	389	50	1,320 (20)
38.39	0.145	363	192	355	22	2,278 (26)	368	31	4,231 (49)	388	25	2,204 (25)
42.96	0.189	363	245	356	23	3,850 (35)	369	30	4,178 (38)	385	50	2,998 (27)
47.44	0.232	362	291	356	24	4,980 (38)	370	30	4,791 (37)	385	51	3,334 (25)
51.86	0.274	362	335	355	23	5,687 (38)	370	29	5,433 (36)	384	52	3,947 (26)
55.58	0.318	362	370	355	23	6,402 (38)	370	28	5,759 (34)	383	51	4,619 (28)
60.93	0.360	361	419	355	23	7,351 (38)	370	28	6,716 (35)	384	51	5,114 (27)
67.41	0.422	361	467	355	23	8,346 (39)	370	28	7,600 (35)	385	53	5,530 (26)
72.95	0.474	361	550	353	22	8,671 (34)	368	27	9,271 (36)	382	50	7,575 (30)
99.01	0.722	361	662	354	24	12,775 (41)	369	28	10,930 (35)	383	52	7,534 (24)

Table 2 Parameters of the deconvoluted Gaussian components of the fluorescence emission of tetracaine (TC.HCl) in aqueous solutions at constant concentration ([TC.HCl]=5.45 μM) in the presence of C_{12}TAB at various micelle concentrations: wavelength λ_i, width W_i, area A_i, and percent contribution to the overall fluorescence emission area (within the parenthesis)

[C_{12}TAB] (mM)	[MIC] (mM)	λ_{max} (nm)	I_{362}	λ_1 (nm)	W_1	A_1 (%)	λ_2 (nm)	W_2	A_2 (%)	λ_3 (nm)	W_3	A_3 (%)
20.37	0.116	367	61	358	26	919 (29)	370	37	1,557 (50)	393	55	649 (21)
22.50	0.153	366	79	358	25	1,291 (34)	370	36	1,822 (47)	393	54	718 (19)
25.04	0.197	365	93	357	24	1,225 (27)	370	32	2,189 (49)	392	51	1,069 (24)
27.92	0.246	364	114	356	23	1,274 (24)	368	31	2,656 (50)	390	49	1,388 (26)
31.06	0.300	364	133	356	23	1,552 (25)	368	31	3,027 (49)	389	49	1,579 (27)
34.39	0.358	363	150	355	22	1,907 (28)	368	31	3,360 (49)	390	49	1,649 (23)
37.85	0.417	363	172	355	23	2,666 (34)	370	30	3,311 (43)	390	48	1,809 (23)
41.38	0.478	363	193	354	22	2,580 (30)	368	29	3,802 (44)	387	47	2,246 (26)
44.92	0.539	362	209	356	23	3,534 (38)	370	30	3,932 (42)	391	48	1,923 (20)
48.43	0.600	362	229	355	23	3,796 (37)	370	30	4,333 (42)	391	48	2,086 (21)
51.87	0.659	362	248	355	22	3,578 (32)	368	30	5,105 (46)	389	47	2,402 (22)
55.23	0.717	362	273	356	23	4,500 (37)	369	31	5,303 (44)	391	48	2,213 (19)
61.58	0.827	362	309	355	22	4,254 (32)	367	30	6,179 (46)	388	47	3,017 (22)
64.55	0.877	362	322	354	22	3,889 (28)	366	29	6,580 (47)	387	46	3,566 (25)
67.38	0.927	362	338	354	21	4,021 (28)	366	29	6,879 (47)	387	47	3,721 (25)

to the emission of the probe immersed in several microenvironments characterized by different hydrophobicity, microviscosity, solvation, etc. [38–42]. Accordingly, the overall emission band of tetracaine in the absence and presence of increasing amounts of OBG and of C_{12}TAB micelles has been deconvoluted after conversion of wavelength to frequency into the optimum number of reproducible overlapping curves (see Figs. 7 and 8 as examples) that have been assigned to different probe environments, bearing in mind that, as long as the hydrophobicity of the solubilizing region increases, the emission becomes more energetic; i.e., the spectral band component is more shifted to lower wavelength. For that purpose, a commercial nonlinear least-squares multi-peaks fitting procedure that uses an iterative Marquardt–Levenberg fitting algorithm, the center, width, and amplitude of each Gaussian curve being the adjustable fit parameters, was used. Several features were chosen as control tests to assure the goodness of the deconvolution: (1) the reproducibility of the final results for the center, width, and amplitude of the peaks, irrespective of the choice of the starting parameters on a series of different fits; (2) a minimum value in the χ^2 parameter; (3) a random residual plot with no systematic features; and (4) a maximum value for the square of the multiple correlation coefficient, r^2, better than 0.999. Tables 1 and 2 resume the fitting parameters for all the experimental spectra of tetracaine in the presence of both nonionic and cationic micelles.

Table 3 Averaged wavelengths and area percentages of the three Gaussian components of the fluorescence emission of tetracaine (TC.HCl) in the presence of OBG and of C_{12}TAB micelles

System	Gaussian band	λ (nm)	Area (%)
TC.HCl+OBG	1	355±2	37
	2	370±2	38
	3	385±3	25
TC.HCl+C_{12}TAB	1	356±2	31
	2	369±3	46
	3	390±3	23

In all the cases, the fitting procedure reveals the presence of three microenvironments that have been assigned as follows: (1) the most red-shifted peak (higher wavelength) has been assigned to the emission of tetracaine in the bulk solution because it is the unique peak that also appears in the fluorescence spectra of tetracaine in pure water. This peak appears at 385±3 nm in the presence of OBG and at 390±3 nm in the presence of C_{12}TAB micelles. This small difference can be explained in terms of the polarity of the media, as the presence of C_{12}TAB monomers and bromide counterions coming from the dissociation of the cationic micelle drives to a more polar media than that one found by tetracaine in a solution with nonionic OBG monomers and micelles. (2) The most blue-shifted peak (lower wavelength) has been attributed to tetracaine inside the hydrophobic core of the micelles. This core is constituted by the hydrocarbon tails of the surfactants and, as it is similar for both nonionic OBG micelles and cationic C_{12}TAB micelles, this peak appears at the same wavelength for both kind of micelles (at 355±2 nm in the presence of OBG micelles and at 356±2 nm in the presence of C_{12}TAB micelles); and finally, (3) the intermediate peak that appears at the same wavelength in the presence of both kind of micelles (at 370±

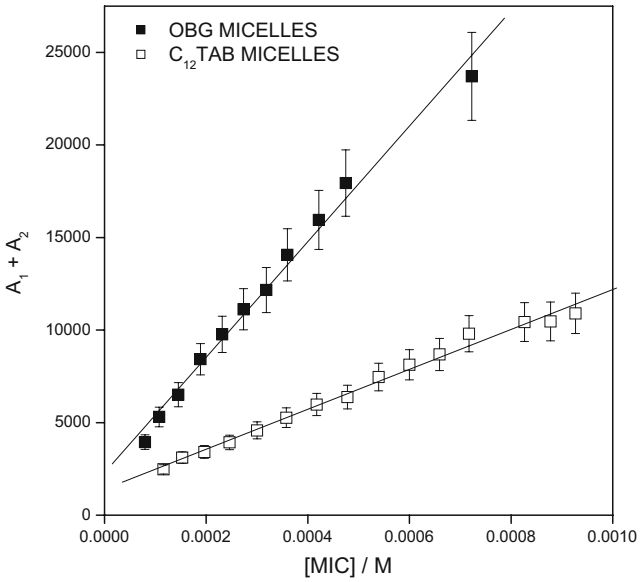

Fig. 9 Plot of (A_1+A_2) vs [MIC], where A_1 and A_2 are the areas of the Gaussian components assigned to tetracaine hydrochloride solubilized within the core and the surface of the micelles, respectively, and [*MIC*] represents the concentration of OBG and/or C_{12}TAB micelles

2 nm in the presence of OBG micelles and at 369±3 nm in the presence of C_{12}TAB micelles) has been assigned to the emission of tetracaine within the micelle surface (see Table 3).

Once the different microenvironments are identified and assigned to wavelengths, attention can be paid to the information yielded by the intensity of the bands in terms of the areas (or as percentages over the total area of the experimental band). Tables 1 and 2 also resume the areas, A_i, of the deconvoluted bands for each emission peak, including the percent contribution to the overall fluorescence emission area. It is well known that there is not a direct correlation between concentration and intensity (or area) of a Gaussian band component assigned to a hydrophobic microenvironment with respect to that assigned a hydrophilic one, as the quantum yield of fluorescence is different in hydrophobic and hydrophilic environments. Thus, for the same probe concentration, fluorescence emission is usually much more intense in hydrophobic media than in an aqueous environment [7]. Accordingly, a larger spectral area of a Gaussian peak that is blue shifted with respect to other is not necessarily correlated with a higher probe concentration within the corresponding microenvironment. But if the Gaussian peak with the larger spectral area is red shifted with respect to the other, a correlation can be established between this intensity (or area) and a higher probe concentration in this more-polar microenvironment. In this case, the quantum yield would be expected to be lower, so a larger area necessarily has to do with a higher probe concentration [7]. In that sense, in view of the averaged area percentages reported in Table 3, we can say that, in the presence of cationic C_{12}TAB micelles, tetracaine drug prefers the surface to the hydrophobic core of the micelles, as $A_2>A_1$ (46 against 31%). In contrast, nothing conclusive can be said about the preferred solubilization site of the drug in the case of OBG micelles because it has been found in Table 1 that $A_1 \approx A_2$ (37 against 38%). In any case, it is worth noticing that tetracaine drug seems to be predominantly solubilized within the micelles (core+surface) in both cases, i.e., $(A_1+A_2) >> A_3$, as can be seen in Tables 1, 2, and 3 (see the percent contribution to the overall fluorescence emission area); it is noticeable that, in both micelle systems, the relation $(A_1+A_2):A_3$ follows a ratio of 3:1, independently of the concentration of micelle aggregates. Also, the evaluation of the sum of the emission areas of the peaks due to the tetracaine solubilized inside, A_1, or in the micelle surface, A_2, helps on the interpretation of the association drug/micelle. Figure 9 shows a plot of (A_1+A_2) vs [MIC] for both OBG and C_{12}TAB micelles. Two features can be concluded from this figure: (a) The roughly linear increase of (A_1+A_2) with the micelle aggregates concentration confirms the drug–micelle association for both non-ionic and cationic micelles, and (b) the increase in (A_1+A_2) is much more accentuated in the presence of OBG aggregates that is in agreement with the values obtained for the association constants $(K_{TCH^+\_OBG} > K_{TCH^+\_C12TAB})$.

Conclusions

This work presents a fluorimetric and conductometric study of the association processes of an anesthetic drug, tetracaine hydrochloride, with two types of micelles: (a) nonionic micelles formed from *n*-octyl-β-D-glucopyranoside (OBG) and (b) cationic micelles formed from dodecyltrimethylammonium bromide (C_{12}TAB). The study not only confirms the association between the drug and both kind of micelles, but also reports a nonlinear method to determine the binding constants. The moderate *K* values obtained for the association of the tetracaine hydrochloride with both nonionic and cationic micelles fall within the optimum range, indicating that both type of micelles are suitable vehicles to solubilize and transport the local anesthetic drug. In particular, OBG nonionic micelles seem to be more appropriate as tetracaine carrier than C_{12}TAB cationic micelles, mostly due to the higher binding constant and the less toxicity of OBG surfactant widely used in biomembrane research. Additionally, the drug–micelles association process has been also analyzed by deconvoluting the overall fluorescence spectra into the optimum number of reproducible overlapping curves that have been assigned to different drug solubilizing environments. In all the cases, the fitting procedure reveals the presence of three microenvironments where the drug is

housed: the bulk solution, the micelle core, and the micelle surface. Nothing conclusive can be said about the preferred solubilization site of the drug in the case of OBG micelles, but in the presence of cationic C_{12}TAB micelles, tetracaine drug prefers the surface to the hydrophobic core of the micelles.

Acknowledgment The authors thank the Spanish Ministry of Education, project no. CTQ2005-1106, and BSCH–UCM Program, project no. PR27/05–14049, for financial support.

References

1. Christian SD, Scamehorn JF (1995) In: Solubilization in surfactant aggregates, vol. 55. Marcel Dekker, New York
2. Somasundaran P, Hubbard A (2002) In: Encyclopedia of surface and colloid science. Marcel Dekker, Santa Barbara, USA
3. Almgren M, Grieser F, Thomas JK (1979) J Am Chem Soc 101:279
4. Atwood JL, Davies JED, MacNicol DD, Vögtle F (1996) In: Comprehensive supramolecular chemistry. Pergamon, Oxford
5. Connors KA (1987) In: Binding constants: the measurement of molecular complex stability. Wiley, New York
6. D'Souza VT, Lipkowitz KB (1998) Chem Rev 98:1741
7. Lakowicz JR (1999) In: Principles of fluorescence spectroscopy. Kluwer, New York
8. Caetano W, Tabak M (1999) Spect Acta A 55:2513
9. Chakraborty H, Roy S, Sarkar M (2005) Chem Phys Lipids 138:20
10. Chakraborty T, Sarkar N (2005) Biophys Chem 117:79
11. Avendaño C (1993) In: Introducción a la Química Farmacéutica. McGraw-Hill–Interamericana, Madrid
12. Bowman WC, Rand MJ (1990) In: Textbook of pharmacology. Blackwell, Cambridge
13. Lopes LB, Scarpa MV, Silva GVJ, Rodrigues DC, Santilli CV, Oliveira AG (2004) Colloids Surf B Biointerfaces 39:151
14. Matos C, Lima GAR, Reis S, Lopes A, Bastos M (2004) Biophys J 86:946
15. Pantos A, Tsiourvas D, Paleos CM, Nounesis G (2005) Langmuir 21:6696
16. Rowat AC, Keller D, Ipsen JH (2005) Biochim Biophys Acta 1713:29
17. Tsogas I, Tsiourvas D, Paleos CM, Giatrellis S, Nounesis G (2005) Chem Phys Lipids 134:59
18. Mehta SK, Bhasin KK, Kumar A, Dham S (2006) Colloids Surf A Physicochem Eng Asp 278:17
19. Helenius A, McCaslin DR, Fries E, Tanford C (1979) Methods Enzymol 56:734
20. Harvie P, Wong FMP, Bally MB (1998) Biophys J 75:1040
21. Michel H, Oesterhelt D (1980) Proc Natl Acad Sci USA 77:1283
22. Baron C, Thompson TE (1975) Biochim Biophys Acta 382:276
23. Stubbs GW, Gilbert SH, Litman BJ (1976) Biochim Biophys Acta 425:45
24. Grip WJ, Bovee-Geurts PHM (1979) Chem Phys Lipids 23:321
25. Cabezas JA, Reglero A, Garcia JI, Rodrigo M, Martinez V, Cabezas M, Fitt H, Hueso P (1989) Jano 37:43
26. Ceccarelli B, Aporti, Finesso M (1976) Adv Exp Med Biol 71:275
27. Hakomori S (1986) Invest Cienc 118:14
28. Ohshima H, Furusawa K (1998) In: Electrical phenomena at interfaces. Fundamentals, measurements, and applications. Marcel Dekker, New York
29. Junquera E, Aicart E (1997) J Phys Chem B 101:7163
30. Junquera E, Peña L, Aicart E (1997) Langmuir 13:219
31. Pastor O, Junquera E, Aicart E (1998) Langmuir 14:2950
32. Junquera E, Aicart E (1999) Int J Pharm 176:169
33. Merino C, Junquera E, Jimenez-Barbero J, Aicart E (2000) Langmuir 16:1557
34. Junquera E, Aicart E (1994) Rev Sci Instrum 65:2672
35. Shinoda K, Yamaguchi T, Hori R (1961) Bull Chem Soc Jpn 34:237
36. Phillips JN (1955) Trans Faraday Soc 51:561
37. Connors KA (1997) Chem Rev 97:1325
38. Karukstis KK (2001) In: Encapsulation of fluorophores in multiple microenvironments in surfactant-based supramolecular assemblies. In: Nanostructured materials, micelles and colloids, vol. 3. Academic, London
39. Karukstis KK, Zieleniuk CA, Fox MJ (2003) Langmuir 19:10054
40. Karukstis KK, McCormack SA, McQueen TM, Goto KF (2004) Langmuir 20:64
41. Aicart E, del Burgo P, Llorca O, Junquera E (2006) Langmuir 22:4027
42. del Burgo P, Aicart E, Junquera E (2006) Appl Spectrosc 60:1307